

## Silicoboron–carbonitride ceramics: A class of high-temperature, dopable electronic materials

P. A. Ramakrishnan and Y. T. Wang

*Department of Physics, University of Colorado, Boulder, Colorado 80309*

D. Balzar

*Materials Science and Engineering Laboratory, NIST, Boulder, Colorado 80303*

Linan An

*Department of Mechanical Engineering, University of Colorado, Boulder, Colorado 80309*

C. Haluschka and R. Riedel

*Fachbereich Materialwissenschaft, Fachgebiet Disperse Feststoffe, Technische Universität Darmstadt, Darmstadt, Germany*

A. M. Hermann<sup>a)</sup>

*Department of Physics, University of Colorado, Boulder, Colorado 80309*

(Received 2 January 2001; accepted for publication 19 March 2001)

The structure and electronic properties of polymer-derived silicoboron–carbonitride ceramics are reported. Structural analysis using radial-distribution-function formalism showed that the local structure is comprised of Si tetrahedra with B, C, and N at the corners. Boron doping of SiCN leads to enhanced *p*-type conductivity ( $0.1 \Omega^{-1} \text{cm}^{-1}$  at room temperature). The conductivity variation with temperature for both SiCN and SiBCN ceramics shows Mott's variable range hopping behavior in these materials, characteristic of a highly defective semiconductor. The SiBCN ceramic has a low, positive value of thermopower, which is probably due to a compensation mechanism. © 2001 American Institute of Physics. [DOI: 10.1063/1.1370540]

Amorphous, nonstoichiometric silicon–carbonitride (SiCN) ceramics show excellent high-temperature structural properties such as oxidation and creep resistance.<sup>1–3</sup> The SiCN ceramics can be conveniently synthesized from inorganic polymers by pyrolysis of the polymer precursor.<sup>4,5</sup> The composition of the polymer-derived ceramics (PDCs) can be designed by choosing the appropriate polymeric precursor. It is also possible to derive a covalent micro/nanocomposite of Si<sub>3</sub>N<sub>4</sub>/SiC by crystallizing the amorphous-SiCN ceramics at high temperatures.<sup>1</sup> This nanocomposite is oxidation resistant at temperatures up to 1600 °C. Owing to their high-temperature stability, the PDCs have been successfully demonstrated for application in microelectromechanical systems.<sup>6</sup>

The SiCN ceramics can be doped with boron using the polymer precursor tris[dichloromethylsilyl]ethylborane.<sup>5</sup> The silicoboron–carbonitride ceramics show excellent stability up to 2000 °C even in nitrogen-free environments. Although the structural and mechanical properties of these ceramics have been investigated in detail, only limited data on the electronic properties of these materials is available. The electrical conductivity of SiCN ceramics derived from polyhydrazinomethylsilane was reported by Scarlete *et al.*<sup>7</sup> A high room-temperature dc conductivity of the order of  $10^4 \Omega^{-1} \text{cm}^{-1}$  was found for these ceramics and was attributed to the fourfold coordinated nitrogen acting as a donor. Recently, Haluschka, Engel, and Riedel<sup>8</sup> reported the electrical properties of SiCN ceramics derived from poly(hydr-

domethyl)silazane and the effect of annealing treatments on the electrical transport properties. These ceramics showed a much lower electrical conductivity compared to those derived from polyhydrazinomethylsilane. Thus, the backbone structure of the polymer influences not only the structure of the ceramics but also the electrical transport properties.

In this letter, we present our studies on the electronic properties of boron-doped SiCN ceramics. We find that boron doping leads to *p*-type conductivity with a dramatic increase in room-temperature conductivity of  $10^{-1} \Omega^{-1} \text{cm}^{-1}$ . For comparison, we also present the electrical resistivity data for the insulating SiCN ceramics annealed at 1300 °C in air.

The silicon–carbonitride and silicoboron–carbonitride ceramics were obtained by pyrolysis of polyhydridomethylsilazane (NCP 200) and tris[dichloromethylsilyl]ethyl borane polymer precursors, respectively. The latter is obtained by hydroboration of dichloromethylvinylsilane using dimethylsulfide borane in the ratio of 2:1 (hence, hereafter referred to as 2:1 polymer). Details of the synthetic procedures have been described elsewhere.<sup>4,5</sup> The structural features of the ceramics were analyzed using x-ray diffraction (XRD). The diffraction data were collected on a commercial two-circle powder diffractometer with Cu *K*α radiation (~8 keV photon energy).

The electrical resistivity of the samples as a function of temperature was measured using a closed-cycle refrigerator. The electrical resistivity of the pristine SiCN ceramics was measured using ac impedance technique, described elsewhere.<sup>9</sup> The resistance values were confirmed by dc measurements using high-input impedance circuitry. For the SiBCN sample, a standard four-probe technique with Ag

<sup>a)</sup>Author to whom correspondence should be addressed; electronic mail: allen.hermann@colorado.edu

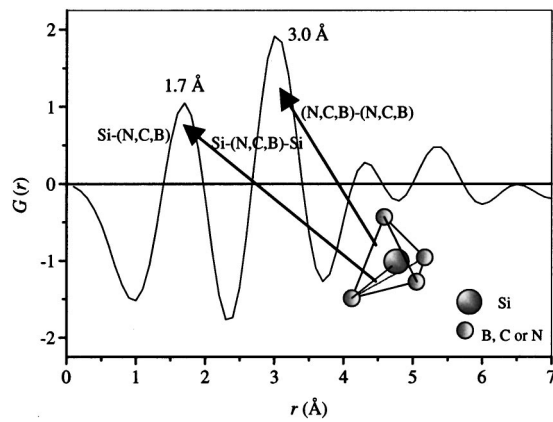


FIG. 1. Reduced radial distribution function  $G(r)$  as a function of correlation distance  $r$  from an arbitrary atom at its origin. The two first maxima correspond to the distances between the central tetrahedral atom (Si) and tetrahedron corners (C, N, or B) and tetrahedron edge lengths, respectively.

electrodes was used. Thermopower was measured by a low-frequency ac technique, described previously.<sup>10</sup>

The as-synthesized pristine ceramic had a composition  $\text{Si}_{1.7}\text{C}_{1.0}\text{N}_{1.6}$ , and is amorphous as revealed by x-ray diffraction. We carried out heat treatments in air and nitrogen at 1300 °C to study the changes in structure and electrical properties. While the sample heated in nitrogen atmosphere did not show any crystalline phase, the sample annealed in air was partially oxidized to form a crystalline  $\text{SiO}_2$  (cristobalite) phase (the XRD pattern showed an amorphous background with reflections of cristobalite). Conversely, the SiBCN sample derived from 2:1 polymer had the composition  $\text{Si}_2\text{BC}_{3.4}\text{N}_{2.3}$  and did not show any crystalline peaks after annealing at 1550 °C in nitrogen, and it appeared amorphous in x-ray diffraction measurements. In general, the amorphous state of boron-doped ceramics can be retained up to temperatures exceeding 1800 °C owing to the retarding effect of boron on the atomic mobilities.

There are no studies on the short-range order in boron-doped SiCN. We, therefore, estimated the short-range order of SiBCN ceramic through a quick study using laboratory x rays and radial distribution function formalism, in order to assess any large differences between SiBCN and previously published SiCN structural data.<sup>11,12</sup> The reduced radial distribution function (RRDF)  $G(r)$  is obtained as a Fourier transform of reduced structure factor (interference function)  $F(Q)$ :

$$G(r) = (2/\pi) \int_0^\infty F(Q) \sin(Qr) dQ.$$

Here,  $F(Q) = Q[S(Q) - 1]$ ,  $S(Q)$  is a structure factor,  $Q = 4\pi \sin \theta / \lambda$ ,  $\theta$  is a scattering angle,  $\lambda$  is a wavelength, and  $r$  is a distance from the atom to an arbitrary atom at the origin.

For highly disordered glasses,  $Q_{\text{max}} \approx 8\text{--}10 \text{ \AA}^{-1}$  generally suffices, but for substantial long range order or crystalline materials it should be significantly extended. Our measurements were done up to  $7.5 \text{ \AA}^{-1}$ , which allows for qualitative assessment of short-range order in SiBCN, which is highly disordered.<sup>5</sup>

The x-ray results are presented in Fig. 1, and the RRDF closely resembles data previously published for SiCN.<sup>11</sup>

Therefore, the short-range structure of SiBCN likely is comprised of Si tetrahedra with B, C and N at the corners (Fig. 1). The first RRDF maximum is given by the Si–N, Si–C, and Si–B distances. Compared to the published results,<sup>11</sup> Fig. 1 shows the first maximum to be slightly shifted toward larger distances, likely because the Si–B distance should be larger than the other two (the distances in Ref. 11 were determined as Si–N=1.74 Å, and Si–C=1.83 Å). If we consider a tetrahedron with an average Si–M (M=N,C,B) bond length of 1.9 Å, the average tetrahedron edge length [ $1.9 \text{ \AA} \times (8/3)^{1/2} \approx 3.1 \text{ \AA}$ ] presents different, B, C, and N interdistances. This corresponds to the second RRDF maximum. Another characteristic correlation contributing to this maximum is the average Si–(N,C,B)–Si second-neighbor distance. Two higher RRDF maxima correspond to larger distances, such as the second-neighbor Si–(N,C,B) distances and the Si–Si distances between C–N or C–B corner-linked neighboring tetrahedra.

Although Fig. 1 qualitatively agrees very well with the RRDF for SiCN,<sup>11</sup> a short-range-order study at much higher energy (59 keV) is under way. At this energy, maximum  $Q_{\text{max}} > 20 \text{ \AA}^{-1}$  are accessible, which yield a significantly more precise RRDF resolution in real space. An improved resolution might allow separation of Si–C, Si–N, and Si–B distances in the first maximum, to help clarify the boron role in doped SiCN.

The pristine SiCN sample resulting from pyrolysis of the polymer at 1000 °C in Ar is an insulator, exhibiting a room-temperature conductivity of  $\sim 10^{-10} (\Omega \text{ cm})^{-1}$ . It is found that the conductivity can be improved drastically (over 8–10 orders of magnitude) by annealing in nitrogen atmosphere at elevated temperatures. However, it may be noted that annealing at temperatures higher than 1300 °C leads to formation of crystalline impurities of SiC and  $\text{Si}_3\text{N}_4$  and, hence, the increase in conductivity of samples annealed at temperatures higher than 1300 °C cannot be thought of as the intrinsic property of the SiCN ceramics. The room-temperature conductivity increased to  $4 \times 10^{-7} (\Omega \text{ cm})^{-1}$  upon annealing at 1300 °C in nitrogen atmosphere.

The sample heated in air at 1300 °C exhibits an ambient temperature conductivity of  $1.5 \times 10^{-7} \Omega^{-1} \text{ cm}^{-1}$ , an increase of three orders of magnitude over the as-pyrolyzed sample, despite partial oxidation leading to cristobalite formation. The increase in conductivity can be rationalized on the basis of loss of hydrogen during annealing at higher temperatures. The loss of hydrogen leads to an increase in the  $sp^2/sp^3$  ratio of the carbon atoms. This leads to lowering of the energy barrier for the transport of charge carriers, and, consequently, to the electrical conductivity increase.

The variation of conductivity with inverse temperature exhibited nonlinear behavior (inset, Fig. 2), which is due to the high density of states within the mobility gap. We found that the conductivity exhibited a linear behavior when plotted against  $T^{-1/4}$ , which is typical of three-dimensional (3D) variable range hopping (VRH)<sup>13</sup> (Fig. 2).

Upon boron doping, the conductivity of the ceramics increased significantly. We show in Fig. 3 the conductivity as a function of temperature for the SiBCN ceramic (2:1) annealed at 1550 °C for 10 h in nitrogen. The sample shows a conductivity as high as  $0.1 \Omega^{-1} \text{ cm}^{-1}$  at ambient tempera-

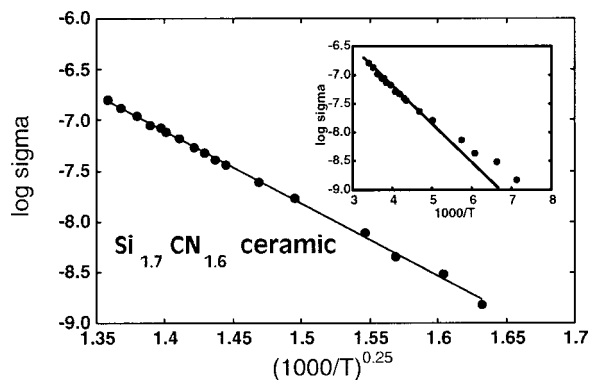


FIG. 2. Conductivity variation with temperature for the SiCN ceramics showing that the three-dimensional VRH mechanism is operative. Inset shows the nonlinear Arrhenius plot for this material.

ture. This conductivity behavior for the B-containing sample was also found to obey Mott's 3D VRH mechanism.

The observation of VRH behavior in these ceramics indicates that these materials as prepared are highly disordered with a high density of localized states in the mobility gap. These localized states are characteristic of unsaturated bonds. Our attempts to observe photoluminescence in these materials were not successful, indicating that the carrier lifetime in these materials is very short, probably due to these localized states in the gap corresponding to dangling bonds.

The resistivity of the SiBCN ceramic is one order lower than that of the SiCN sample annealed at 1550 °C in nitrogen. Since the ratio of Si:C:N in the SiCN ceramic is different from that in the SiBCN ceramic, we cannot infer at present that the lower resistivity of the SiBCN ceramic is due to boron doping alone. Although the SiBCN sample remained amorphous after annealing, and the x-ray diffraction pattern did not show any secondary phase formation, probing of the local structure by high-resolution transmission electron microscopy (HRTEM) is necessary to exclude the possibility of formation of graphitic tissue on the nanoscale. Furthermore, there are reports of the evolution of the nanocrystalline Si<sub>3</sub>N<sub>4</sub>, SiC and turbostratic BN(C) phases upon annealing at elevated temperatures.<sup>14</sup> Further spectroscopic, HRTEM, and structural studies using high-energy synchro-

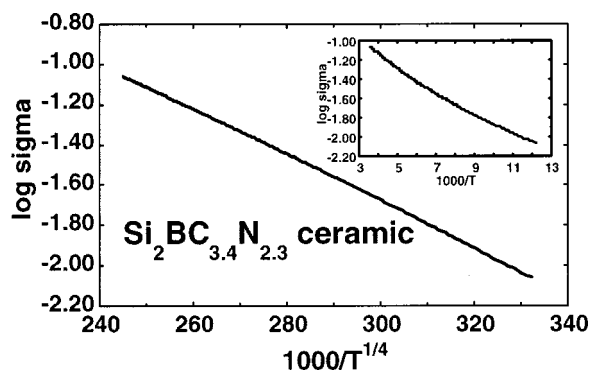


FIG. 3. Conductivity variation with temperature for the SiBCN ceramics showing that the three-dimensional VRH mechanism is operative. Inset shows the nonlinear Arrhenius plot for this material.

tron radiation are underway to clarify these issues.

The SiBCN ceramics (2:1) exhibit very low, positive thermopower ( $\sim 1 \mu\text{V/K}$ ), which is almost temperature independent. We attribute the low, temperature-independent thermopower value to a compensation mechanism. The pristine SiCN ceramic exhibits a low, negative thermopower<sup>8</sup> and this is visualized as due to group-V nitrogen dissolution in a group-IV SiC network. The addition of boron leads to the creation of holes which compensate for the *n*-type doping by nitrogen in the network.

In summary, a preliminary investigation of the short-range order of the SiBCN ceramic shows that the local structure resembles that of SiCN, comprised of Si tetrahedra with B, C, and N at the corners. The conductivity of these ceramics increases dramatically by annealing at elevated temperatures, due to the loss of hydrogen (present in the polymer precursor). The SiBCN ceramics have significantly higher conductivity ( $\rho=10 \Omega \text{ cm}$  at room temperature) than the SiCN ceramics ( $\rho\sim 10^7 \Omega \text{ cm}$ ). The high conductivity combined with excellent high-temperature stability makes these classes of ceramics potential candidates for a variety of high-temperature electrical applications such as high-temperature filaments and conducting coatings. The conductivity variation with temperature follows Mott's VRH mechanism, indicating that these ceramics are highly disordered with unsaturated bonds, resulting in a high density of localized states in the mobility gap. If the defects can be removed (e.g., by saturation of dangling bonds with the introduction of hydrogen or fluorine during processing or during postpyrolysis), fabrication of high-temperature electronic devices based on *pn* junctions would be possible.

<sup>1</sup>R. Riedel, H.-J. Kleebe, H. Schoenfelder, and F. Aldinger, *Nature (London)* **374**, 526 (1995).

<sup>2</sup>L. An, R. Riedel, C. Konetschny, K.-J. Kleebe, and R. Raj, *J. Am. Ceram. Soc.* **81**, 1349 (1998).

<sup>3</sup>R. Riedel, L. Ruwisch, L. An, and R. Raj, *J. Am. Ceram. Soc.* **81**, 3341 (1998).

<sup>4</sup>R. Riedel, G. Passing, H. Schoenfelder, and R. J. Brook, *Nature (London)* **355**, 714 (1992).

<sup>5</sup>R. Riedel, A. Kienzle, W. Dressler, L. Ruwisch, J. Bill, and F. Aldinger, *Nature (London)* **382**, 796 (1996).

<sup>6</sup>L. An, W. Zhang, V. M. Bright, M. L. Dunn, and R. Raj, *Proceedings of the 13th Annual International Conference on Microelectromechanical Systems* (2000), p. 619.

<sup>7</sup>M. Scarlete, J. He, J. F. Harrod, and I. S. Butler, *NATO ASI Ser., Ser. E* **297**, 125 (1995).

<sup>8</sup>C. Haluschka, C. Engel, and R. Riedel, *J. Eur. Ceram. Soc.* **20**, 1365 (2000).

<sup>9</sup>K. J. Rao, N. Baskaran, P. A. Ramakrishnan, B. G. Ravi, and A. Karthikeyan, *Chem. Mater.* **10**, 3109 (1998).

<sup>10</sup>A. M. Hermann, U. Onbasli, R. F. Tello, W. Kiehl, A. Naziripour, and Y. Wang, *Proceedings of the 4th Asian Conference on Solid State Ionics* (1994), p. 37.

<sup>11</sup>J. Bill, J. Seitz, G. Thurn, J. Duerr, J. Canel, B. Z. Janos, A. Jalowiecki, D. Sauter, S. Schempp, H. P. Lamparter, J. Mayer, and F. Aldinger, *Phys. Status Solidi A* **166**, 269 (1998).

<sup>12</sup>F. Ténégal, A.-M. Flank, M. Cauchetier, and N. Herlin, *Nucl. Instrum. Methods Phys. Res. B* **133**, 77 (1997).

<sup>13</sup>N. F. Mott and E. A. Davis, *Electronic Processes in Noncrystalline Materials* (Clarendon, Oxford, U.K., 1979).

<sup>14</sup>A. Jalowiecki, J. Bill, F. Aldinger, and J. Mayer, *Composites* **27A**, 717 (1996).